Self-Diffusion in Core-Shell Composite $^{12}CO_2/^{13}CO_2$ Nanoparticles

Sigurd Bauerecker*

Institut für Physikalische und Theoretische Chemie, Technische Universität Braunschweig, D-38106 Braunschweig, Germany
Institut für Küstenforschung, GKSS-Forschungszentrum GmbH, D-21502 Geesthacht, Germany

(Received 12 August 2004; published 27 January 2005)

A new technique for the generation of multilayered molecular nanoparticles is presented. Core-shell composite nanoparticles of CO_2 with varied composition have been investigated by Fourier-transform infrared spectroscopy over 600 s at 78 K. The isotopically different zones of the particles turned out to have completely different spectra in the ν_3 region: a tub structure (mantle) and a head-and-shoulders structure (core). From the aggregation behavior of both components the particle formation time was found to be 0.1 s. Low-temperature self-diffusion of airborne molecular nanoparticles has been monitored for the first time. The self-diffusion coefficient for $^{12}CO_2/^{13}CO_2$ nanocomposites at 78 K was determined from the time evolution of the $\nu_1 + \nu_3$ combination band to about 7×10^{-20} m^2/s. The work represents a major advance toward nanoengineering of molecular nanoparticles at low temperatures.

DOI: 10.1103/PhysRevLett.94.033404 PACS numbers: 36.40.Sx, 36.40.Mr

Airborne molecular nanoparticles are of considerable importance in atmospheric, medical, and technological fields [1]. To investigate processes of small molecular particles in the time scale of seconds to hours [2,3] collisional cooling techniques in combination with Fourier-transform infrared (FTIR) spectroscopy have become effective methods [4–9]. These processes comprise shape evolution, phase transitions, binary diffusion, and chemical and physical reactions of the particles. While studying and even nanoengineering of colloidal systems with components like latex, metals, metal oxides, or polymers are rapidly developing fields of research [10,11], multicomponent molecular nanoparticles formed at lower temperatures [12] remained largely unexplored.

In this Letter we describe the formation process and the time evolution of composite $^{12}CO_2/^{13}CO_2$ nanoparticles in the gas phase with initial stages ranging from a well separated mantle-core two-phase system to a completely isotopically mixed one-phase system. As we will show, there is strong evidence that the evolution of the combination-band spectra is the result of binary diffusion of the isotopically different mantle molecules into the core region and vice versa. Further, the ν_3 antisymmetric stretching vibration band serves as a reliable indicator of the *macroscopic* particle structure (core-mantle composition, particle shape) while the $\nu_1 + \nu_3$ (and the $\nu_3 + 2\nu_2$) combination band provide *microscopic* structure information of the particles (environment of a single molecule).

The composite $^{12}CO_2/^{13}CO_2$ particles were generated in a collisional cooling long-path cell [9] using a novel multiple gas-pulse inlet technique (Fig. 1). Two quantities of sample gases are rapidly injected through two inlet tubes into the cold buffer gas of the cooling cell where clustering occurs. An electric multiple-pulse generator controls the lengths and repetition frequencies of the gas pulses and especially the time difference (10^{-3} to 10^4 s) between the gas pulses of different inlet channels by electromagnetic valves. This multiple-pulse arrangement allows to bring up to five sample-gas pulses into interaction, each adjustable in volume, prepressure, repetition frequency, and time offset to pulses of the other injection channels. In that way, the composition of multilayered particles or specially coated particles in the nanometer and micrometer size range is possible. The particles are monitored by FTIR spectroscopy with an integrated White optics over 600 s or longer.

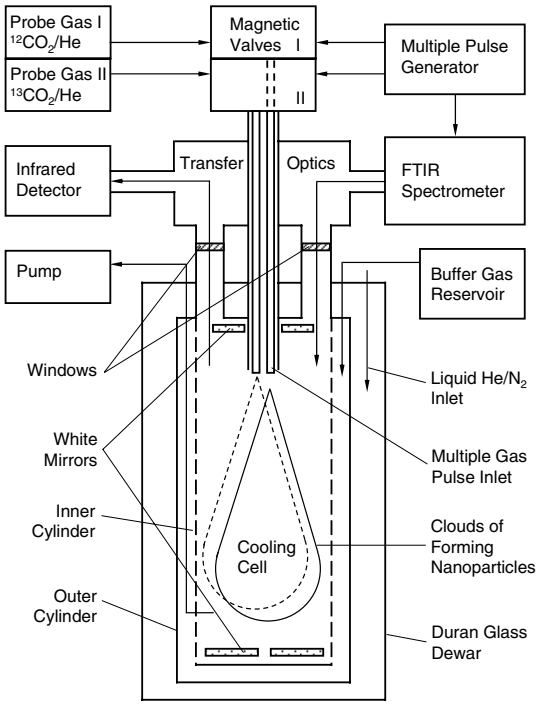

FIG. 1. Schematic view of the experimental setup, including a long-path cooling cell and a new multiple gas-pulse inlet system for the generation of composite particles. The first sample-gas pulse forms the cores of the nanoparticles, the second pulse condenses a mixing layer and/or a well separated mantle on the cores depending on the time difference between the pulses.

In the present experiment one $^{12}CO_2$ (1000 ppm in He) and one $^{13}CO_2$ (1002 ppm in He) gas pulses were injected, each with a volume of 50 ml at a prepressure of 2 bar ± 10% at 297 K. In any case the buffer gas in the cell was Helium at a pressure of 200 mbar, a total volume of 11 dm^3 and a temperature of 78 K. The mirrors were heated to 83 K to avoid CO_2 deposition. The optical parameters were: 1 cm^{-1} spectral resolution; 15 m optical path length; 5 s (60 s for background) recording time of FTIR spectra, 5, 25, 60, 180, 360, and 600 s after injection of the second gas pulse, at 90% saturated InSb detector. The absorbance of the main ν_3 band was about 0.6 at the beginning of recording and decreased by half after 600 s in each case. The *time difference* τ between the $^{12}CO_2$ and the $^{13}CO_2$ pulse was varied from 2.5 to −2.5 s.

First, the effect of τ on the particle composition is discussed. Figure 2 shows a series of spectra of composite nanoparticles in the region of the antisymmetric ν_3 stretching vibration and of the $\nu_1 + \nu_3$ combination band. In the case of trace 1 and two ($\tau = 2.5$ and 0.5 s), the $^{12}CO_2$ molecules of the first pulse cloud have sufficient time to complete homogeneous nucleation before the $^{13}CO_2$ molecules of the second pulse cloud enter the system, aggregate inhomogeneously on the $^{12}CO_2$ nanoparticles and form the mantle layer. The composite nanoparticles are suspended in the cooling cell and can be observed over minutes (up to about 1 h) in thermal equilibrium. In trace 3 the nucleation of the $^{12}CO_2$ molecules has just finished when the $^{13}CO_2$ molecules come into contact with the forming nanoparticles. A mixing peak (MP) at the combination bands starts developing (see arrow) which means that some of the $^{12}CO_2$ molecules start coaggregating with the $^{13}CO_2$ molecules at about $\tau = 0.1$ s. Therefore, it can be concluded that the formation of the particles (cores) is being completed within about 0.1 s. The mixing portion increases with decreasing τ (trace 4 to 8) and reaches perfect coaggregation at $\tau = 0$ s in trace 9 where the sample-gas fractions of both pulse clouds have been completely mixed before nucleation. In the four bottom spectra ($\tau = -0.02$, -0.1, -0.5, and -2.5 s) the pulse order has been reversed. Here, the nuclei are formed by $^{13}CO_2$ molecules and the mantles by $^{12}CO_2$ molecules.

Some of the spectroscopically relevant information on CO_2 nanoparticles formed by collisional cooling at our experimental conditions are summarized: The main size (diameter) of the particles in this work has been estimated from Mie scattering theory to 110 nm [3] in accordance with Ref. [2]; the structure is crystalline face-centered cubic (Pa3) [6,13–16]; their IR spectra of the ν_2 and ν_3 band extend between the transverse (TO) and the longitudinal (LO) optical mode of the crystal and are strongly affected by the particle shape via the resonant coupling mechanism of the oscillating molecular dipoles in the aggregate [2,16–18].

A striking feature of Fig. 2 is the pronounced difference between the $^{13}CO_2$-mantle and the $^{12}CO_2$-core spectra in the ν_3 region for $|\tau| > 0.05$ s, see trace 1 to 4 (and 11 to 13 with reversed isotopomer composition). Especially in view of temporal behavior the spectra turn out to develop reproducibly toward a *tub structure* for the mantle and a *head-and-shoulders structure* for the core, see trace 1 in Fig. 3. To exclude that a physical effect of the second sample-gas pulse on the forming composite nanoparticles, such as a small heat input, is responsible for this asymmetry, the following pulse combinations have been thoroughly investigated as control experiments: $^{12}CO_2$/He, $^{12}CO_2/^{12}CO_2$, He/$^{12}CO_2$, $^{13}CO_2$/He, $^{13}CO_2/^{13}CO_2$, and He/$^{13}CO_2$. The experiments clearly show that these six

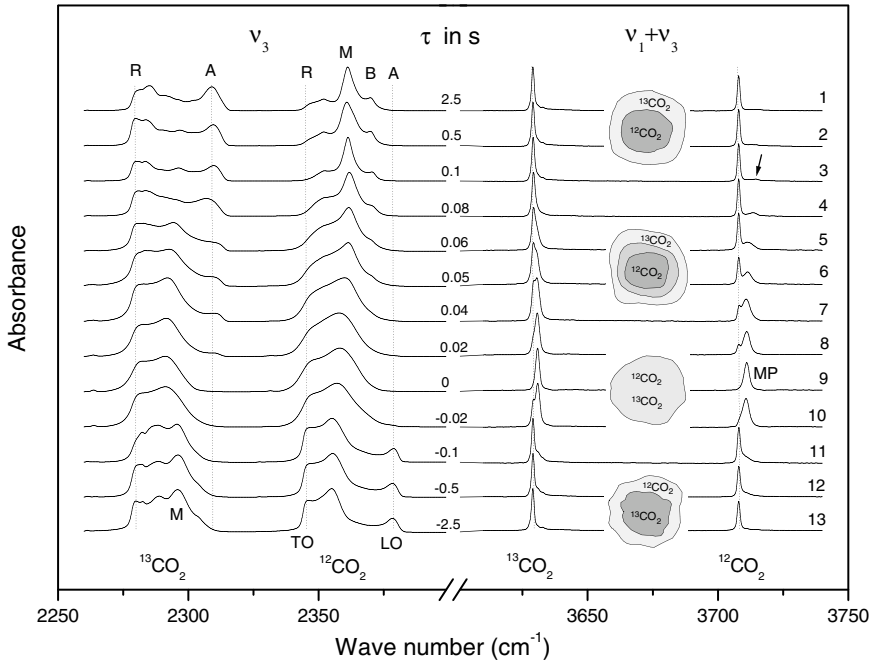

FIG. 2. FTIR spectra of $^{12}CO_2/^{13}CO_2$ composite nanoparticles forming in mixing aerosol clouds of $^{12}CO_2$/He and $^{13}CO_2$/He which were injected into the cooling system with a time difference ranging from $\tau = 2.5$ s ($^{12}CO_2$ pulse first) to -2.5 s ($^{13}CO_2$ pulse first). Recording started 5 s after injection of the second pulse. The different composition of the particles is schematically illustrated. The MP of the $\nu_1 + \nu_3$ combination band (see arrow) indicate the portions of molecules with isotopically mixed vicinities.

ν_3-band spectra and their temporal behavior only slightly differ. They all have the typical structure and temporal development of trace 14 in Fig. 3, shown as an example.

The "core spectra" of the $^{12}CO_2$-related ν_3 region (trace 1 to 4 between 2344 and 2381 cm^{-1} in Fig. 2) are similar to the spectra of pure CO_2 nanoparticles with the difference of a suppressed *R* peak (compare ν_3 region in trace 1 and 14 in Fig. 3). In contrast, the "mantle spectra" of the $^{13}CO_2$-related ν_3 region (trace 1 to 4 between 2278 and 2312 cm^{-1} in Fig. 2) do not show the head-and-shoulders structure of the pure CO_2 nanoparticles but rather a tub structure. Most prominent is the occurrence of a further spectral feature in the case of the composite particles, labeled with an *A* in Figs. 2 and 3, at 2309.0 cm^{-1} and 2378.5 cm^{-1} for the $^{13}CO_2$ and $^{12}CO_2$ mantles (trace 1 to 4 and 11 to 13 in Fig. 2, trace 1 and 11 in Fig. 3). To our knowledge, the *A* feature has not yet been described in literature as a spectral feature of CO_2 *nanoparticles* but as a feature of *molecular films* or *slabs* of CO_2 (and N_2O) and has been assigned to the LO mode [2,17,19–21] ($\nu_{LO} = 2381$ cm^{-1} and $\nu_{TO} = 2344$ cm^{-1} for $^{12}CO_2$) [17]. Therefore, if we view the molecular mantle of the nanoparticles as a hollow sphere or a curved film, then the *A* peak can be interpreted as an LO mode absorption of the infrared light. This result is in agreement with detailed investigations of layers of CF_4 molecules on water-ice particles with varied thickness [12].

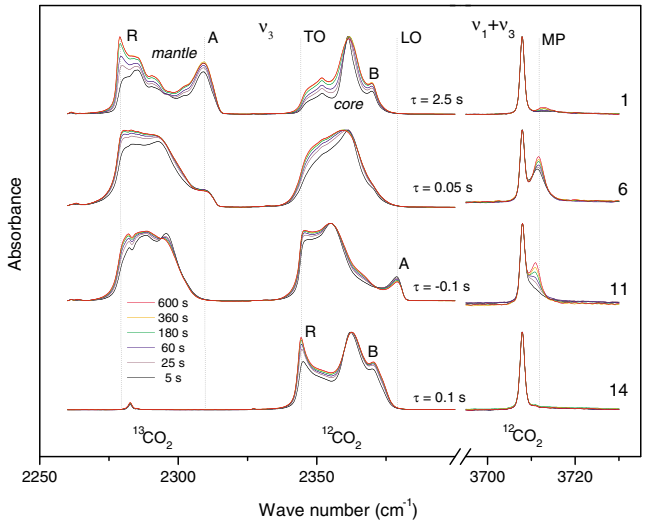

FIG. 3 (color online). Temporal evolution of three selected IR spectra of Fig. 2 (trace 1, 6, and 11) over 600 s and of a comparative spectrum resulting from a control experiment with a $^{12}CO_2$/He pulse followed by a pure He pulse after 0.1 s (trace 14). Note that the mantle in trace 1 contains both TO and LO structures (*R* and *A* peak) after ripening, typical for a hollow sphere. The portion of molecules with isotopically mixed vicinities increases over 600 s by self-diffusion of both isotopomers, see MP of the $\nu_1 + \nu_3$ combination band. In each series, the spectra extend from inside/bottom (black) to outside/top (red/gray) with time.

Compared to the main ν_3 vibrations the less intense $\nu_1 + \nu_3$ combination bands of $^{12}CO_2$ and $^{13}CO_2$ are not sensitive to the macroscopic particle features like shape and size. On the other hand, they are suitable indicators of the order of state and the microscopic composition [3,22,23]. In our experiments additional spectral features, labeled with MP, occur a few wave numbers blueshifted from the combination-band peaks, resulting from CO_2 molecules embedded in an environment containing molecules of the other isotopomer, e.g., see arrow at the $\nu_1 + \nu_3$ band of $^{12}CO_2$, trace 3 to 12 in Fig. 2. The relative intensity of this mixing peak increases up to 100% when complete mixing of both isotopomers is reached at $\tau = 0$ s. The corresponding peak has its maximum at 3711.0 cm^{-1} and its width (FWHM) is with 2.4 cm^{-1} twice the width of the peak of the pure component in trace 1. The redshift of the mixing-peak position from 3714.6 to 3711.0 cm^{-1} (trace 3 to 10) can be assigned to environments with different $^{13}CO_2$ fractions ranging from 7% to 63% in accordance to Ref. [21]. The corresponding mixing-peak position of the $^{13}CO_2$ molecules is 40% to 50% less blueshifted from the peak of the pure component at 3629.0 cm^{-1} than in the $^{12}CO_2$ case and therefore both peaks are less separated, (trace 3 to 10). Summarizing, we can get two different pieces of information from the mixing peak of the combination bands: (a) the relative integrated absorbance gives a measure of the relative volume of the mixing zone in the particles and (b) the position of the MP indicates the mean molar fractions of the isotopomers in the mixing zone.

The temporal behavior of the spectral *hook* structure at the TO mode of the ν_3 band of pure CO_2—see trace 14 in Fig. 3—has been frequently discussed [2,3,6,9,15,23–27] and recently explained by shape evolution of the nanoparticles [3,16]. However, it remained an open question whether longish particles agglomerate from globular primary particles or if the globular primary particles themselves change to longish particles by dendritic growth [16]. With the results presented in Fig. 3 the situation can be further clarified. The comparison of mantle and core in trace 1 clearly shows that only the mantle and not the core contributes to the growing *R* peak. Furthermore, the barely changing *A* peak indicates that the particles keep a layered structure. Therefore, it is unlikely that the particles *themselves* evolve to longish ones like needles.

In the following discussion we focus on the $\nu_1 + \nu_3$ combination-band evolution. Most striking, especially in trace 6 and 11 of Fig. 3, is the relative growth of the MP over the period of 600 s, while the main peak of the pure component at 3708 cm^{-1} remains unchanged in its shape. In Fig. 4 the mixing-peak evolution is depicted for different τ. We interpret this behavior as one-dimensional self-diffusion driven by concentration gradients of both isotopomers in the CO_2 nanoparticles. To estimate the diffusion coefficient *D*, we examine the time evolution of the spectrum with maximum pulse interval $\tau = 2.5$ s which ensures completed formation and cooling of the particle

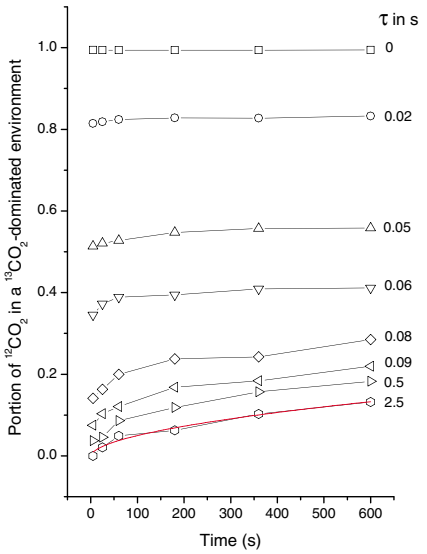

FIG. 4 (color online). Increase over time of the mixing zone in core-shell composite CO_2 nanoparticles caused by self-diffusion. The initial thickness of the isotopically mixed layer decreases with time interval τ between aggregation of the sample-gas clouds of both isotopomers. In the case of $\tau = 2.5$ s, self-diffusion starts from a well zone-separated $^{12}CO_2$-core/$^{13}CO_2$-mantle composite: the data points can be fitted by a root function with the exponent of 0.55 (red/gray solid curve), according to the theory of one-dimensional self-diffusion.

cores prior to condensation of the mantle and thus an approximately steplike concentration gradient between core and mantle at the beginning of the self-diffusion process. After $t = 600$ s, the mixing zone (portion of $^{12}CO_2$ in a $^{13}CO_2$-dominated environment) has grown to 13.2% of the integrated absorbance of the combination band. From our results presented in Figs. 2 and 3 it follows that roughly the same absorbance per molecule for isotopically pure and mixed regions can be assumed. The width of the mixing zone can be approximated from Fick's second law using the mean-square net-displacement z perpendicular to the boundary area between core and mantle: $z = \sqrt{2Dt}$. An even better approximation is $z_0 = \sqrt{\pi Dt}$, see Ref. [28]. With a mean particle diameter of 110 nm, we get an estimation of $D \approx 7 \times 10^{-21}$ m^2/s $\pm$ 50%. This corresponds with the lower range of typical self-diffusion coefficients of solids [28]. The lowest self-diffusion coefficients for carbon dioxide we could find in the literature are such for fluid carbon dioxide at 223 K and 200 MPa with about 2.1×10^{-9} m^2/s [29] being 11 to 12 orders of magnitude higher than ours.

A more detailed analysis of the determination of binary diffusion data from the spectroscopy of layered nanoparticles remains the subject of a future study. Anisotropy effects and temperature dependence of D should be also investigated. In any case, the comparison of the experimental data with exciton model and molecular dynamics calculations is planned. It is worth mentioning that, if one reverses the line of argumentation, it should be possible to obtain particle size information from calibrated diffusion data of solid and fluid composite particles, too.

The author thanks J. Reichardt for fruitful comments.

*Email address: s.bauerecker@tu-bs.de

[1] W. C. Hinds, *Aerosol Technology* (John Whiley & Sons, New York, 1999).
[2] R. Disselkamp and G. E. Ewing, J. Chem. Phys. **99**, 2439 (1993).
[3] M. K. Kunzmann, R. Signorell, M. Taraschewski, and S. Bauerecker, Phys. Chem. Chem. Phys. **3**, 3742 (2001).
[4] J. K. Messer and F. C. De Lucia, Phys. Rev. Lett. **53**, 2555 (1984).
[5] J. A. Barnes, T. E. Gough, and M. Stoer, Rev. Sci. Instrum. **60**, 406 (1989).
[6] T. E. Gough and T. Wang, J. Chem. Phys. **105**, 4899 (1996).
[7] R. F. Niedziela, M. L. Norman, C. L. DeForest, and R. E. Miller, J. Phys. Chem. A **103**, 8030 (1999).
[8] J. P. Devlin, C. Joyce, and V. Buch, J. Phys. Chem. A **104**, 1974 (2000).
[9] S. Bauerecker, M. Taraschewski, C. Weitkamp, and H. K. Cammenga, Rev. Sci. Instrum. **72**, 3946 (2001).
[10] F. Caruso, in *Nano-Surface Chemistry*, edited by M. Rosoff (Marcel Dekker, New York, 2002), p. 505.
[11] F. Caruso, Adv. Mater. **13**, 11 (2001).
[12] V. Buch, L. Delzeit, C. Blackledge, and J. P. Devlin, J. Phys. Chem. **100**, 3732 (1996).
[13] G. Torchet, H. Bouchier, J. Farges, M. F. de Feraudy, and B. Raoult, J. Chem. Phys. **81**, 2137 (1984).
[14] L. S. Bartell, Chem. Rev. **86**, 491 (1986).
[15] F. Fleyfel and J. P. Devlin, J. Phys. Chem. **93**, 7292 (1989).
[16] R. Signorell and M. K. Kunzmann, Chem. Phys. Lett. **371**, 260 (2003).
[17] M. A. Ovchinnikov and C. A. Wight, J. Chem. Phys. **99**, 3374 (1993).
[18] R. Signorell, J. Chem. Phys. **118**, 2707 (2003).
[19] D. A. Dows and V. Schettino, J. Chem. Phys. **58**, 5009 (1973).
[20] O. Berg and G. E. Ewing, Surf. Sci. **220**, 207 (1989).
[21] M. K. Kunzmann, Doctoral Thesis, Cuvillier Verlag, Göttingen, 2002.
[22] T. E. Gough and T. Wang, J. Chem. Phys. **102**, 3932 (1995).
[23] M. K. Kunzmann, S. Bauerecker, M. A. Suhm, and R. Signorell, Spectrochim. Acta, Part A **59**, 2855 (2003).
[24] G. E. Ewing and D. T. Sheng, J. Phys. Chem. **92**, 4063 (1988).
[25] J. A. Barnes, T. E. Gough, and M. Stoer, J. Chem. Phys. **95**, 4840 (1991).
[26] M. L. Clapp and R. E. Miller, Icarus **105**, 529 (1993).
[27] A. Bonnamy, M. Jetzki, and R. Signorell, Chem. Phys. Lett. **382**, 547 (2003).
[28] W. Jost, *Diffusion* (Steinkopff, Darmstadt, 1957).
[29] T. Groß, J. Buchhauser, and H.-D. Lüdemann, J. Chem. Phys. **109**, 4518 (1998).